

Ultrahigh-Average Power Solid-State Laser

John Vetrovec*

The Boeing Company

6633 Canoga Avenue, Canoga Park, CA 91309, USA

ABSTRACT

This work presents an improved disk laser concept, where a diode-pumped disk is hydrostatically clamped to a rigid substrate and continuously cooled by a microchannel heat exchanger. Effective reduction of thermo-optical distortions makes this laser suitable for continuous operation at ultrahigh-average power.

Keywords: solid-state lasers, disk laser, active mirror, beam quality

1. BACKGROUND

The key challenge for developing high-average power (HAP) solid-state lasers (SSL) are thermomechanical distortions caused by waste heat deposited into the gain medium by optical pumping. Removal of waste heat leads to thermal lensing, mechanical stresses, depolarization, and other effects, with likely consequences of degraded beam quality (BQ), reduced laser power, and a possible fracture of the SSL medium [1]. In particular, transverse temperature gradients ($\nabla_{\perp}T$) (i.e., perpendicular to laser beam axis) cause thermal lensing. The three principal SSL configurations for bulk gain medium are rod, zigzag slab, and disk, Figure 1.


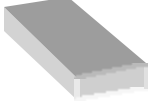

Challenge	 Rod	 Slab (zigzag)	 Disk
Thermal Lensing	Significant (can be compensated except for bi-axial focusing)	None in y-z plane (zigzag path averages out $\nabla_{\perp}T$), weak in x-z plane	None (1-D heat flow eliminates $\nabla_{\perp}T$)
Stress Birefringence	Significant (can be compensated)	None (for ideal slab with 1-D heat flow)	None (1-D heat flow)
Mode Control	Generally good at lower avg. power	More difficult with increasing aspect ratio	Good
Modal Fill Factor for TEM ₀₀	up to ~80% (95% goal)	up to 78%	up to ~95%
Best Power with Good BQ	500 W @ M ² ~ 1.5 [2]	3 kW @ M ² ~ 2.4 [5]	13 kW @ M ² ~ 4 [11]

Figure 1: Principal configurations of SSL gain medium and their comparison

Rod lasers are very susceptible to radial temperature gradients that are responsible for thermal lensing and depolarization due to thermal stress-induced birefringence [ibid]. Both effects can be compensated (at least in smaller devices) and, as result, rod lasers generating good quality beams (M² ~1.5) with over 500 W of average power were recently reported by Boeing-LLNL team [2].

The zigzag slab laser overcomes most of the limitations of the rod laser. In an ideal (infinite) slab, stress-induced birefringence is eliminated by one-dimensional (1-D) heat flow offered by the rectangular geometry. The zigzag path averages out $\nabla_{\perp}T$ and thus eliminates thermal and stress-induced focusing [3]. However, a finite-size slab experiences weak lensing in the transverse direction (parallel to slab width). In principle, average power of the slab scales with the slab width. Unfortunately, a slab with a large aspect ratio (width/height) permits propagation of certain higher order modes resulting in a degraded beam quality. Improved mode control of a HAP slab laser can

* jan.vetrovec@boeing.com; tel. 1 818 586-3101, fax 1 818 586-3074

be achieved with a master oscillator-power amplifier (MOPA) architecture but only at the expense of increased size, complexity, and cost [4]. In addition, the beam fill factor for TEM₀₀ mode in the rectangular aperture is at best 78% ($\pi/4$), which intrinsically limits slab amplifier efficiency. Furthermore, portions of the slab from which power is not extracted are a prime environment for amplified spontaneous emission (ASE) and parasitics. Diode-pumped slab lasers with BQ ~ 2.4 and average power output around 3 kW have been recently reported by TRW [5]. Innovations such as addition of undoped end caps [1], longitudinal pumping [6, 7], and use of ytterbium [8] continue to improve the slab laser but its further scaling to higher average power with good BQ appears very challenging.

Disk lasers have been considered since the early days of SSL development. In a disk gain medium, $\nabla_{\perp}T$ are largely avoided because waste heat is extracted from the disk in the direction parallel to laser beam axis. Because of this 1-D heat flow, disk lasers enjoy inherently low susceptibility to thermal lensing and stress birefringence. In addition, their large, round aperture reduces diffraction and beam clipping losses experienced by other SSL configurations. Disk lasers have demonstrated lasing at HAP with very good BQ [9,10]. In a recent experiment a flash-lamp pumped Nd:glass disk laser generated over 13 kW of average power [11]. Planned upgrade of this device to diode pumping and Nd:GGG disks is expected to allow lasing in a time-limited (heat capacity mode) at about 100 kW. These developments, in combination with advances in diode pumping architectures, crystal growing, new lasing materials, and cooling technologies, are driving a renewed interest in disk lasers.

2. DISK LASERS

As seen in Figure 2, a disk laser may use "transmissive" disks or "reflective" disks. In a transmissive disk, waste heat is removed by gas flowing through the laser beam path. Extensive investigations of transmissive disk cooling suggest that under practical conditions, the maximum achievable heat transfer rates are about 5 W/cm² [12]. In a reflective disk, also known as active mirror amplifier (AMA), the back surface of the disk is available for liquid cooling, which can be applied more uniformly, can easily handle heat fluxes around 100 W/cm², and is well suited for continuous operation at HAP.

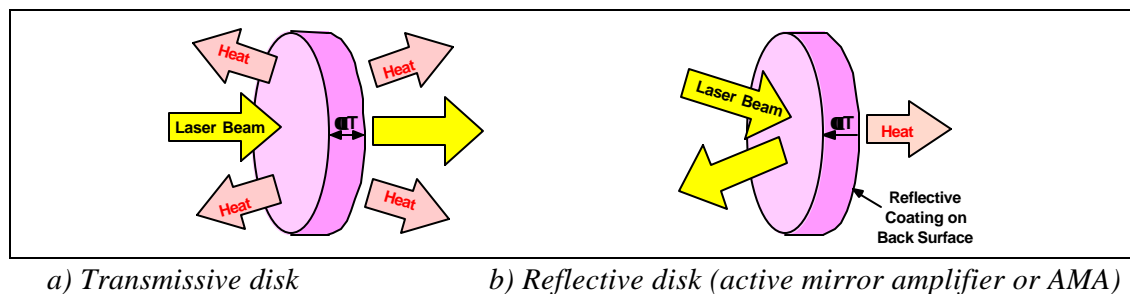


Figure 2: Architectures for cooling disk lasers

Both disk laser types (transmissive and reflective) have been in development since the late 1960s, especially as amplifiers for giant pulse lasers for inertial confinement fusion at the Lawrence Livermore National Laboratory (LLNL) and other research establishments [13]. Active mirror disk was originally developed by General Electric in the late 1960s and used in large-scale, single-shot laser systems at the University of Rochester [14,15]. In the classical AMA concept, a large diameter (~ 25 cm), edge-suspended, Nd-glass disk several centimeters thick, is pumped by flashlamps and cooled by liquid on the back face, Figure 3. The front face has a dichroic coating that is antireflective at laser wavelength and reflective for the pump, whereas the back face has a dichroic coating with opposite properties. However, the classical AMA is unsuitable for HAP operation because of poor heat removal and lack of control over thermally-induced warping. Previous attempts to mitigate these problems and increase the average power output of flash lamp-pumped AMA produced only limited results [16,17].

In recent years, the active mirror disk has been investigated in Germany in the form of a "thin disk laser" [18] schematically shown in Figure 4. Thin disk laser uses a Nd:YAG or Yb:YAG laser crystal disk ~ 3 mm in diameter and 200 to 400 μm in thickness soldered to a heat sink. Diode-pumped Yb:YAG thin disk laser with two disks has

demonstrated laser outputs approaching 1 kW average power and with beam quality $M^2 \sim 12$ [19]. Another variant of the thin disk laser intended for multi-kW outputs is investigated at LLNL [20]. However, owing to its small dimensions, cumbersome pump architecture, and extremely high heat fluxes, thin disk laser does not appear easily scalable in power to much beyond a few kilowatts. Figure 5 shows a comparison of major disk laser concepts classified according to the mode of operation.

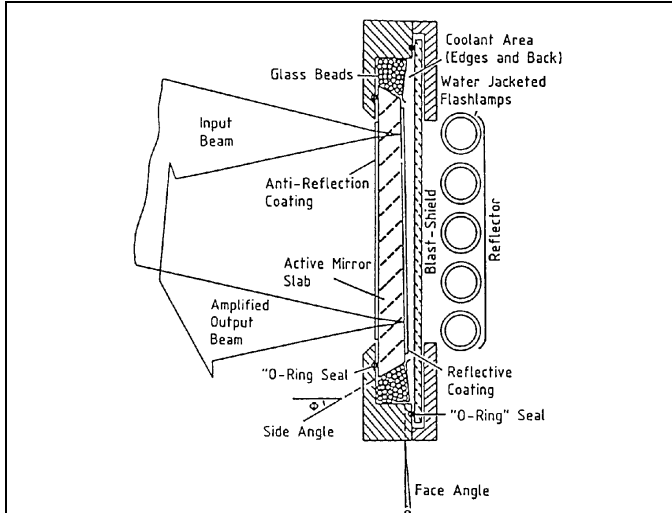


Figure 3: AMA for high-peak power [14]

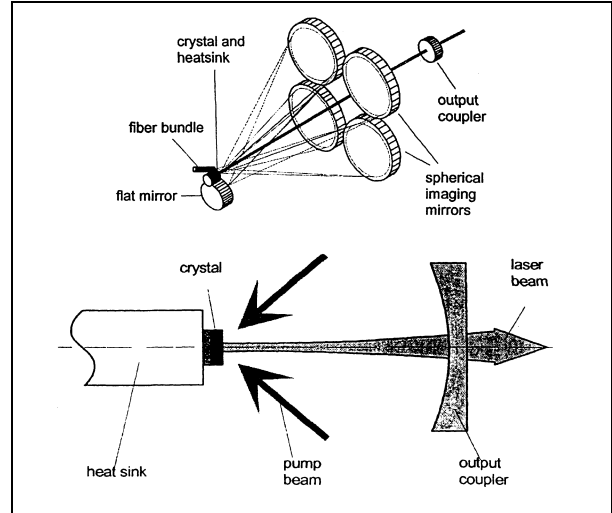


Figure 4: Thin disk laser [18]

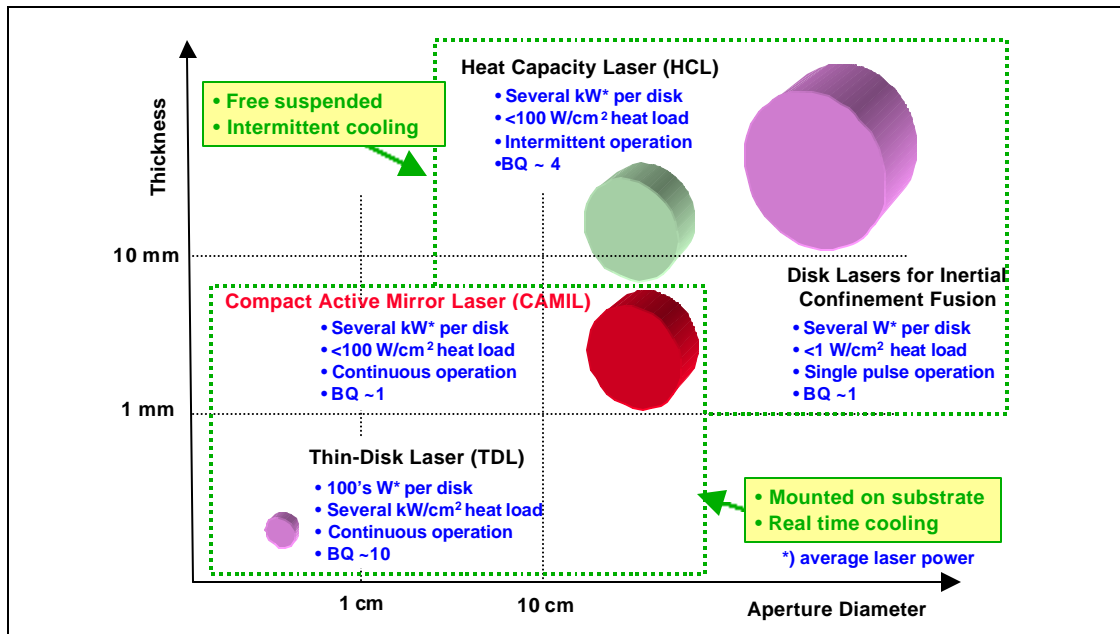


Figure 5: Comparison of major disk laser types classified according to mode of operation

3. COMPACT ACTIVE MIRROR LASER (CAMIL)

The first test of diode-pumped Nd:GGG active mirror disk was conducted at Boeing in 1992 [21, 22]. Over the last several years, Boeing has been developing a disk laser known as the Compact Active Mirror Laser (CAMIL) [23,24]. CAMIL combines disk laser geometry with diode pumping, cooling by a microchannel heat exchanger, and pressure clamping that effectively mitigates thermally induced deformations experienced in earlier disk lasers. In CAMIL, the gain medium disk with 1 to 3 mm thickness and with a diameter typically between 3 and 15 cm is mounted on a rigid, cooled substrate, Figure 6. Gain media suitable for construction of the disk include Nd:YAG,

Nd:GGG, Nd:glass, Yb:YAG, Yb:S-FAP, and Yb:GGG. The substrate contains a built-in heat exchanger with microchannels on the front surface so that coolant can directly wet the back face of the laser medium disk. The disk is clamped to the substrate by a hydrostatic pressure differential between the surrounding atmosphere and the coolant fluid in the microchannels. Hence, the substrate acts as a "backbone" that keeps the disk in optically flat condition. This novel approach provides uniform cooling at high heat flux and effectively suppresses thermal deformations of the disk. With the disk acting as a laser amplifier, high-average power laser oscillator can be constructed by placing 10 to 20 modules into a conventional unstable resonator such as shown, for example, in Figure 7.

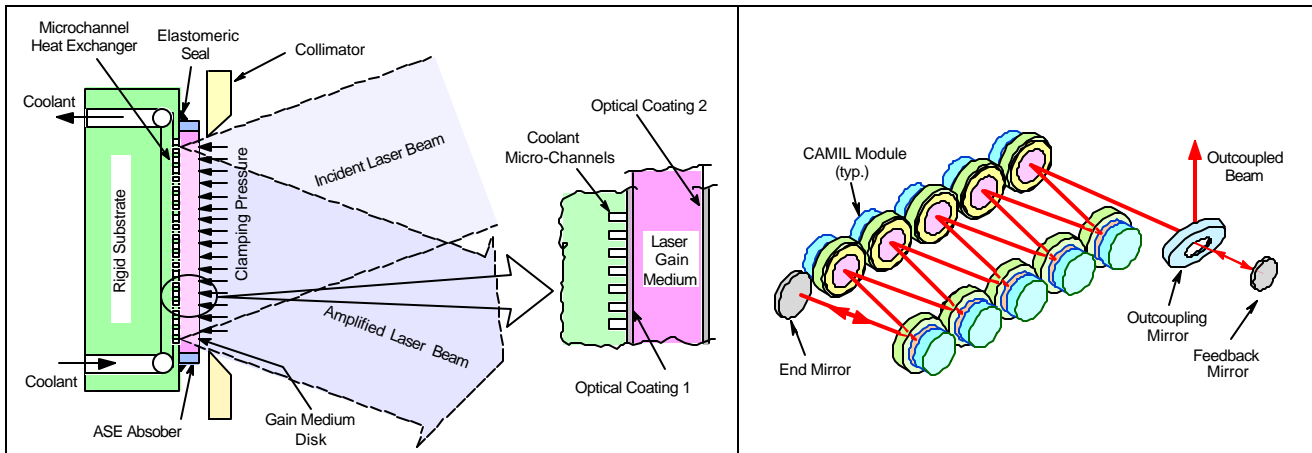


Figure 6: CAMIL concept

Figure 7: CAMIL oscillator

4. PUMP ARCHITECTURES

Pump radiation can be injected into the disk either through one of the large faces (face-pumping) or through the peripheral edge (side-pumping). Face-pumping (FP) can be implemented with diode power injected into the back face of the disk (facing the substrate) as shown in Figure 8, or the front face of the disk as shown in Figure 9. In the former case, the substrate is made of material optically transparent at pump diode wavelength (e.g., fused silica [25,26]). Both disk faces have dichroic coatings: (1) the front face coating is antireflective at laser wavelength and reflective at pump wavelength, and (2) the rear surface coating has the opposite properties. Collimated diode array output is injected into the disk through the substrate and the heat exchanger.

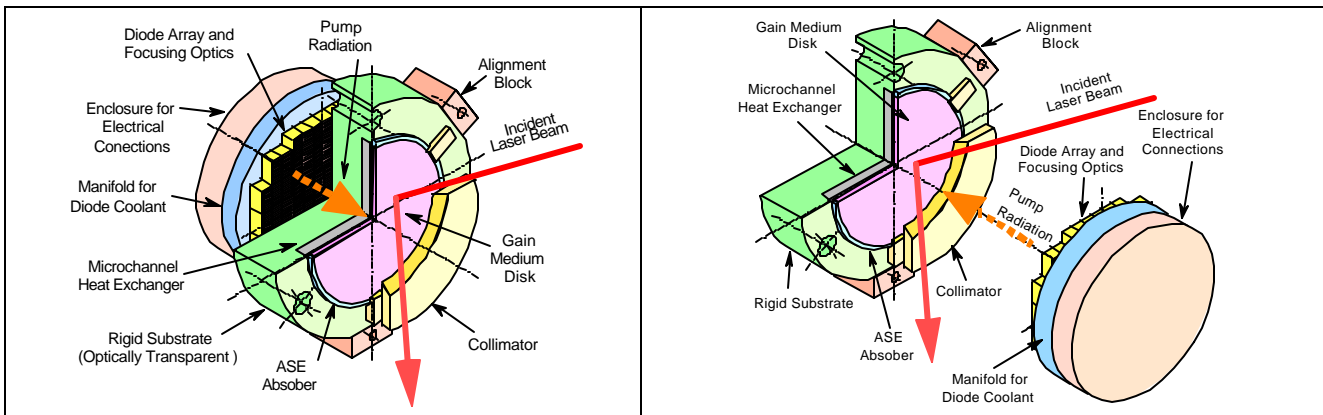


Figure 8: CAMIL module with back face pumping

Figure 9: CAMIL module with front face pumping

Host material of the disk is doped with lasant ions so that about 90% of the pump power is absorbed in two passes through the medium. Front-injected CAMIL operates in a similar way as the back-injected version, but it does not

require a transparent heat exchanger. However, in the front-injected configuration, the diode arrays compete for space with the laser beam. In addition, temperature gradient inside the front-injected disk is about 20% steeper than in a back-injected disk operated under the same conditions.

Face-pumping can be impractical for materials with a low absorption cross-section because the short absorption path (two times disk thickness) forces the designer to specify higher doping. In such situations, injecting the pump radiation into the disk side (i.e., peripheral edge) becomes an attractive alternative. Side-pumping (SP) takes advantage of the long absorption path (approximately same dimension as disk diameter), which permits doping the disk with reduced concentration of lasing ions. This consideration is of critical importance for some very desirable gain media.

Side-pumped CAMIL, shown in cross-section in Figure 10 and in the exploded view in Figure 11, uses a composite disk produced by diffusion bonding of undoped crystal to the peripheral edges of a doped crystal disk. This construction improves coupling between the pump diodes and the gain medium, aids concentration of pump radiation, draws heat away from disk edge, and helps to suppress parasitic oscillations by providing a trap for amplified spontaneous emission (ASE) [24]. Diode pump arrays are arranged around the circumference of the composite disk pointing toward its center and inject pump radiation into the peripheral edge of the disk. If necessary, concentrator ducts and lensing elements can be added to further intensify the pump [ibid]. Aided by multiple internal reflections, pump radiation is channeled into and through the doped portion of the disk where it is gradually absorbed. In Section 7 of this article we will show that by balancing the position and focusing of pump diode arrays with pump adsorption, it is possible to uniformly pump the gain medium disk over the entire aperture. Figure 12 summarizes the key aspects of the three pump architectures. Figure 13 identifies the suitability of several laser gain media for use with face pumping and side pumping architectures.

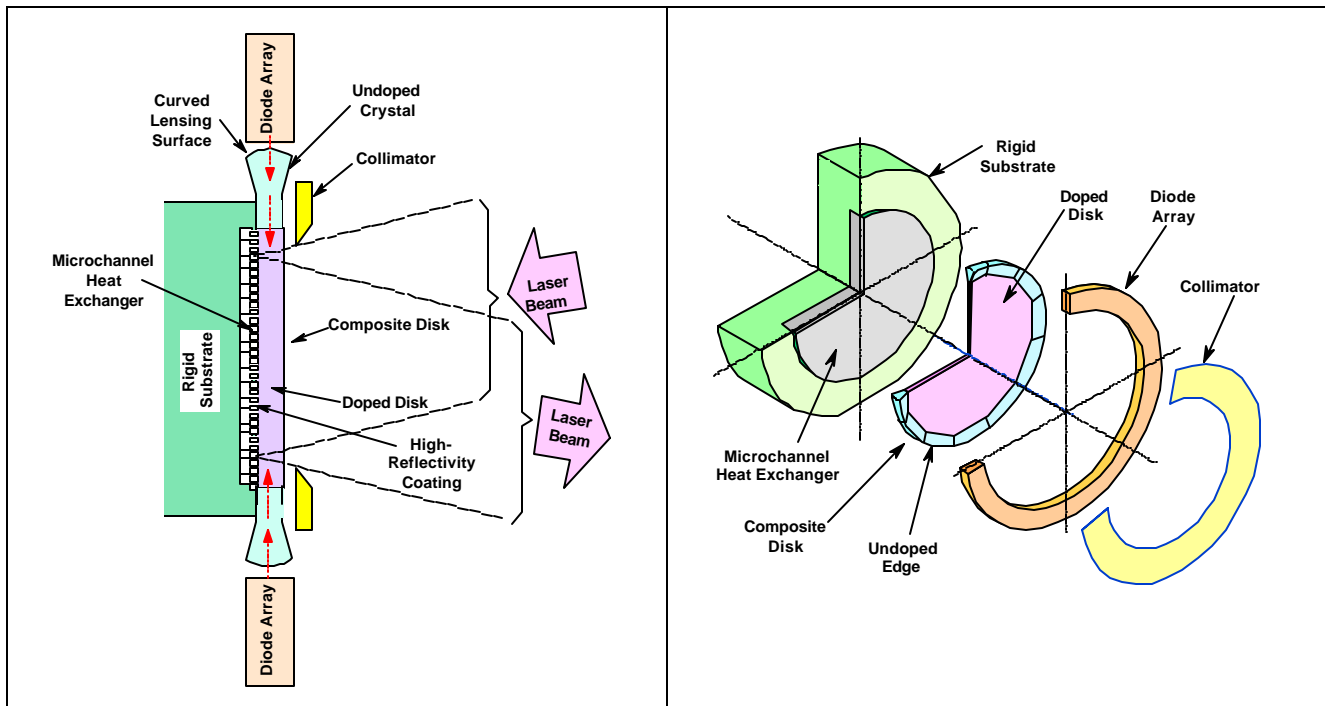


Figure 10: Cross-section of side-pumped CAMIL

Figure 11: Side-pumped CAMIL: exploded view

	Coatings	Heat Exchanger and Substrate	Diode Array Placement	Disk Construction	ASE / Parasitics Suppression	Absorption Path
Front Face-Pumping	High-reflection/ antireflective	Can be opaque	Competes for space with laser beam	Monolithic	ASE absorption claddings	2 times disk thickness
Back Face-Pumping	Dichroic	Transparent	Good	Monolithic	ASE absorption claddings	2 times disk thickness
Side-Pumping	High-reflection / antireflective	Can be opaque	Excellent	Composite	ASE trap	~ 1 time disk diameter

Figure 12: Comparison of pump architectures

	Nd ³⁺						Yb ³⁺		
	YAG		GGG		ED-2 Glass		YAG	GGG	S-FAP
Pump Wavelength [nm]	808	885	808	885	808	880	941	941	905
Absorption Cross-Section [10 ⁻²⁰ cm ²]	6.2	1.2*	1.9	-0.5**	2.2	~1	0.8	~0.4***	9.9
Suitable for Face-Pumping	√		√		√	√			√
Suitable for Side-Pumping		√	√	√	√	√	√	√	

*) Estimated based on data in [28] **) Estimated **) [29]

Figure 13. Suitable pump architecture for several SSL materials

5. AVERAGE POWER SCALING

One key advantage of CAMIL is its scalability over a broad range of average laser powers [27]. In particular, power scaling can be accomplished by increasing the aperture size and/or by increasing the number of modules in a laser oscillator, as shown for the face-pumped CAMIL in Figure 14.

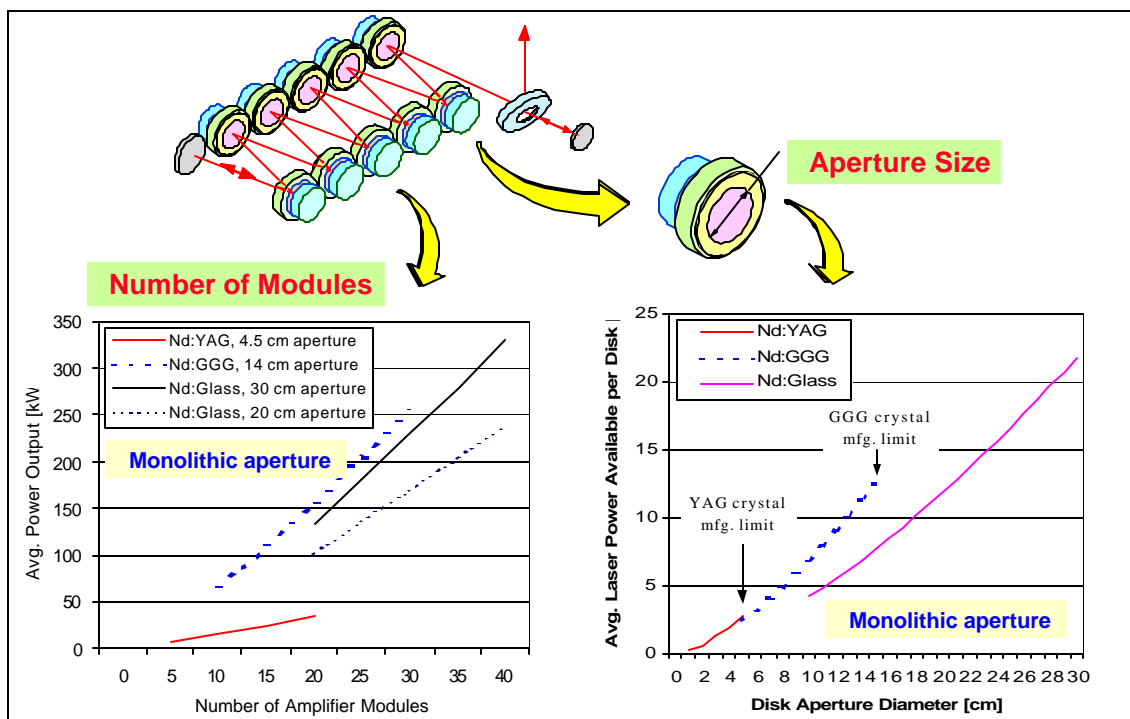


Figure 14: Power scaling of face-pumped CAMIL with number of amplifier modules and disk aperture size

For any given aperture size, the maximum average laser power is also limited by thermal fracture of the gain medium and by ASE losses. For a 4-level system we have shown that in the regime limited by thermal fracture and ASE, the maximum average laser power in the disk that is available for outcoupling ($P_{\text{avail,avg,max}}$) is given by [23]

$$P_{\text{avail,avg,max}} = (\pi/4) (3\mathfrak{R}b\eta_u I_{\text{sat}} \psi_d \phi d^3 f_h^{-1})^{1/2} \quad (1)$$

where \mathfrak{R} is a thermal stress resistance parameter, b is a stress factor (ratio of the design tensile stress and the fracture stress on the cooled surface, typically chosen between 0.25 and 0.5), η_u is the upper state efficiency of the gain medium (a product of Stokes and quantum efficiencies), I_{sat} is the laser saturation intensity, ψ_d is the pump duty factor (= pump pulse length multiplied by pulse frequency), ϕ is an ASE parameter which primarily depends on the mode of operation ($\phi \sim 2.5$ for storage mode and ~ 3.5 for cw or quasi-cw), d is the disk diameter, f_h is the heat fraction (= heat induced per absorbed pump energy). Similar expression can be derived for a quasi-3 level laser [24]. Note that equation (1) is independent of the pump architecture, but it includes all the pertinent spectroscopic and thermo-mechanical parameters of the gain medium.

Size of a monolithic disk is generally limited by the maximum available size of a monolithic laser gain medium, which is about 5 cm for Nd:YAG and about 15 cm for Nd:GGG. A 5-cm Nd:YAG disk pumped by 808 nm light can generate around 2.5 kW of average laser power available for outcoupling ($P_{\text{avail,avg}}$). This suggests that Nd:YAG is suitable for constructing lasers for up to about 50 kW of average power. To attain higher output, the number of required Nd:YAG amplifier stages becomes increasingly impractical and the designer should consider larger disks to keep the system well-balanced. A 15-cm Nd:GGG disk pumped by 808 nm light can generate around 12 kW $P_{\text{avail,avg}}$. Nd:GGG has spectroscopic and thermo-mechanical properties comparable to Nd:YAG, but GGG crystals tolerate higher doping with Nd^{3+} ions and are available in better quality. As seen in Figure 14, a laser producing over 100-kW can be constructed with only about 16 face-pumped Nd:GGG disks.

Nd:glass is also suitable for construction of powerful HEL. In contrast to crystals, Nd:glass is very inexpensive, is available in large sizes (up to 100 cm) and in a superior quality. Furthermore, Nd:glass has a broader absorption line at around 808 nm (~ 20 nm wide vs. ~ 2 nm for Nd:YAG), which relaxes thermal control requirements for the pump diodes and allows for a more robust system. A 15-cm Nd:glass disk can produce about 7 kW $P_{\text{avail,avg}}$ when pumped by 808-nm light.

6. PRESSURE CLAMPING

The gain medium disk is clamped to the substrate by a hydrostatic pressure differential between the surrounding atmosphere and the coolant fluid in the heat exchanger microchannels. In this fashion, the substrate acts as a "backbone" that keeps the disk in an optically flat condition, Figure 15. We derived the following expression for rough estimating the pressure differential Δp_{clamp} required to maintain the disk of diameter d and thickness L in flat condition when operating in the regime limited by ASE and thermal fracture [23]:

$$\Delta p_{\text{clamp}} = 16 (L/d)^2 b \sigma_{s,\text{fract}} / (5+\nu) \quad (2)$$

where b is the stress factor defined earlier, $\sigma_{s,\text{fract}}$ is the fracture stress of the material, and ν is the Poisson ratio.

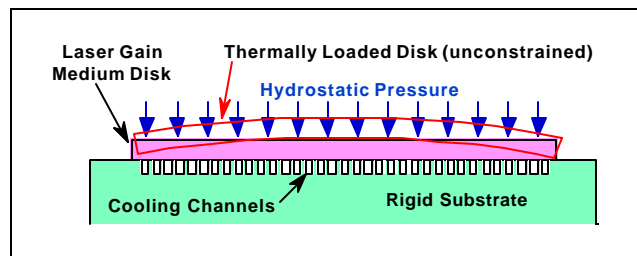


Figure 15: Hydrostatic clamping concept

In most cases of practical interest, Δp_{clamp} is less than 100 psi. To investigate the relationship between optical flatness of a thermally loaded disk and applied hydrostatic pressure we developed a 3-dimensional NASTRAN^{®a} finite element model. Figure 16 shows the results of numerical simulations for a GGG disk indicating that the residual warping effect (“wrinkle”) is confined to the disk edge. By increasing the clamping pressure the wrinkle can be literally “ironed out.” This means that nearly 100% of the pumped volume is available for power extraction.

Figure 17 shows front surface displacement and deformations predicted by the finite element model for a 15-cm Nd:GGG disk pumped to 25% fracture limit. It is evident that the central portion of the disk remains flat even as the material has undergone thermal expansion. Therefore, this portion of the disk provides no net impact on optical path difference. However, a small region around the disk edge is deformed both because of temperature gradients and imperfect clamping. The diameter of the central portion of the disk where displacement is under 0.2 μm is about 12.5 cm. This means that over 92% of the pump disk volume is suitable for power extraction with low optical aberration.

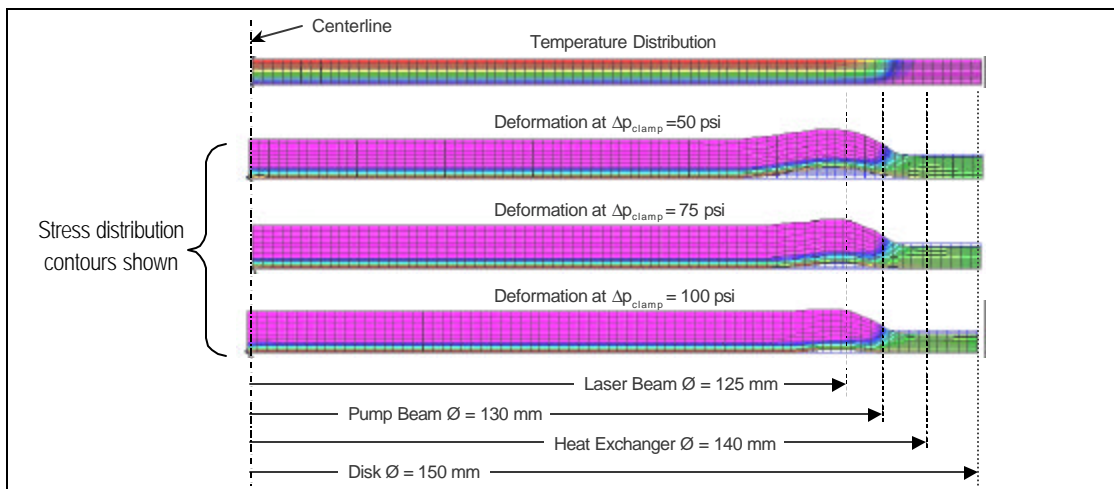


Figure 16: Residual deformations of the disk near the edge are flattened by increasing pressure (expansion of the disk and deformations are exaggerated in vertical direction)

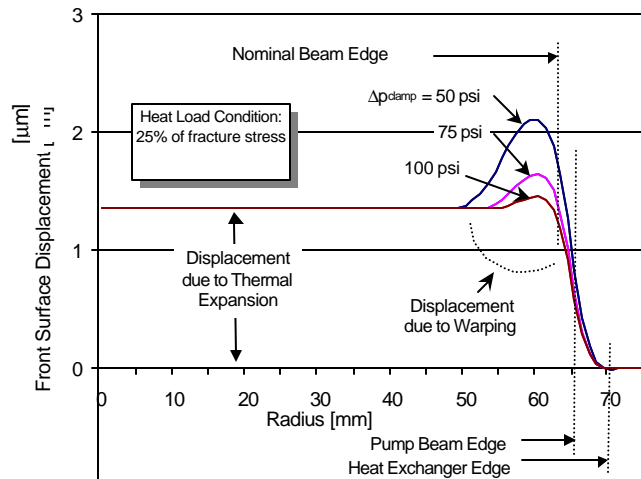


Figure 17: Front surface displacement and deformations predicted by the model for a 15-cm Nd:GGG disk (13-cm beam aperture) pumped to 25% fracture limit

^a McNeal-Schwendler Corp., Pasadena, CA, USA

Pre-forming the disk to a shape opposite to anticipated deflection can significantly reduce required Δp_{clamp} [30]. As an alternate approach to pressure-clamping, we are investigating the possibility of diffusion bonding the gain medium to the substrate. Such bonds with optical coating sandwiched between two optical elements have been successfully demonstrated for small contact area ($\sim 1 \text{ cm}^2$) [31].

7. ADVANCED CONCEPTS

Direct Pumping of Neodymium

Neodymium ion Nd^{3+} is traditionally pumped by diodes on the 808-nm absorption line that has a large cross-section, as seen for example, for Nd:YAG in Figure 18. Yet, the performance of Nd^{3+} can be greatly improved by energy deposition directly into the upper lasing level. The direct pumping scheme shown in Figure 19 uses the absorption feature in the vicinity of 885 nm.

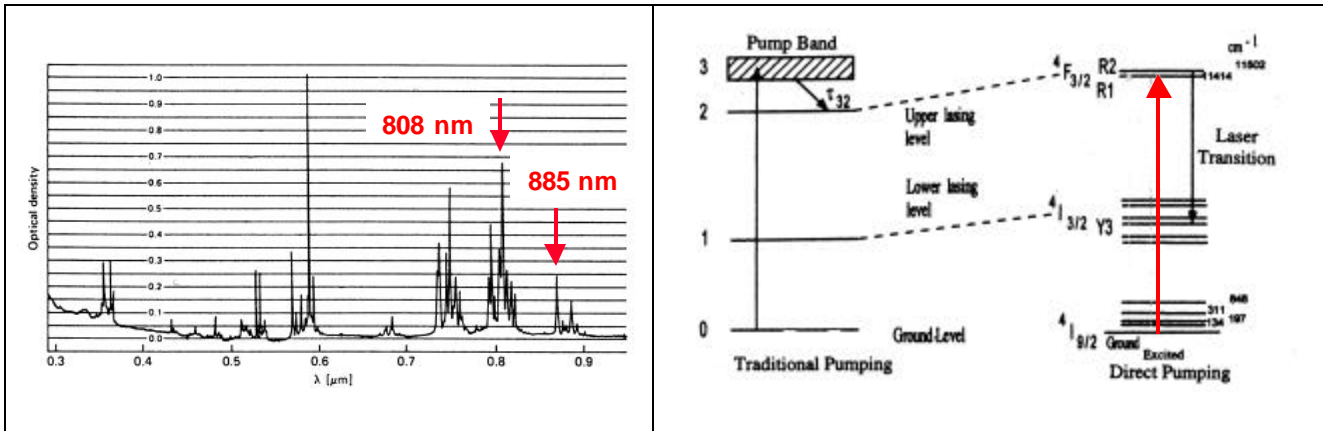


Figure 18: Absorption spectrum of Nd^{3+} in YAG [31]

Figure 19: Energy levels of Nd^{3+} in YAG [28]

Feasibility of direct pumping has been established in the 1960's. However, the small cross-section of the absorption feature at 885 nm (about 3 times smaller than the absorption line at 808 nm) in combination with the lack of sufficiently bright pump sources made direct pumping impractical at that time. Introduction of diode pumping and commercial availability of narrow band diodes emitting 885 nm light [32,33] are changing this situation. Direct pumping improves Stokes efficiency by nearly 10% and entirely avoids the quantum efficiency loss ($\sim 5\%$) associated with energy transfer from the pump band to the upper lasing level. Using direct pumping, Lavi et al. [28] recently demonstrated Nd:YAG laser with 53% optical-optical efficiency. The same work showed that direct pumping can reduce waste heat fraction (f_h) by about 30% and improve electric efficiency of the laser by about 10%.

In view of the small absorption cross-section and Nd doping limit in YAG and GGG crystals, direct pumping is viable only with crystal configurations offering long absorption length, for example a side-pumped disk. Unlike in YAG where the 885 nm the absorption feature is about 2.5 nm wide (about the same as the 808 nm line), in GGG and glass the absorption feature is almost 20 nm wide. This has a major operational implication as it relaxes the tolerances on diode operating temperature by almost eight-fold and allows for a more robust system. Note that glass can be doped to a much higher level that permits direct-pumping to be used with the face pumping architecture.

Ytterbium Lasant

Much of recent research in SSL has been devoted to ytterbium (Yb^{3+}) lasant that has an emission spectrum in the vicinity of $1 \mu\text{m}$ [25]. Interest in ytterbium is primarily motivated by its low Stokes shift, which translates to a low heat fraction (f_h). Depending on the absorption line and host medium crystal used, the heat fraction for Yb-based

system can be several times smaller than for Nd:YAG pumped on the 808 nm line. In practice, this means that a Yb-doped disk could be pumped harder and potentially generate two to three times higher output than a Nd-doped disk using the same host material and diameter. Other advantages of Yb³⁺ over Nd³⁺ include long fluorescence lifetime and simple energy-level structure (only two levels: ground state and excited state) that prevents excited state absorption, up-conversion, and concentration quenching. For high-average power applications, thermomechanical properties of laser crystals are a major consideration. Today, the most important host crystals for high-average power Yb laser are YAG and GGG. Yb:YAG and Yb:GGG can be conveniently pumped at the broad absorption feature around 941 nm or, alternately, at the zero-phonon line around 970 nm. A diode-pumped Yb:YAG disk laser in active mirror configuration pumped by 941 nm diodes demonstrated 58% optical-to-optical efficiency [19]. Recently, a group of French researchers operated Yb:GGG laser pumped by 971 nm light at the zero-phonon line and lased at 1,022 nm, which translates to Stokes efficiency ~95% [29].

In many host crystals of practical interest (e.g., YAG and GGG) Yb³⁺ has rather small pump cross-sections. This makes face-pumping impractical because high doping would be required to provide efficient pump absorption. That in turn would necessitate very high pump intensities to overcome re-absorption of laser radiation by the ground energy state. For example, at ambient temperature, a 2.5 mm-thick YAG disk would require over 4% atomic doping concentration of Yb³⁺ ions to absorb 90% of face-injected pump radiation in two passes. Such a high concentration of Yb³⁺ ions would require impractically high pump density of about 7 kW/cm³ to induce medium transparency and several times this level to efficiently operate the laser. In addition, high doping greatly reduces thermal conductivity of YAG [36]. Happily, this situation is resolved with side-pumping, where the long absorption path (~disk diameter) allows reduced doping and only moderate pump intensities. For example, a 3-cm diameter Yb:YAG disk would require about 0.6% doping to absorb 90% of side-injected 941-nm pump radiation at pump density 1,100 W/cm³ required to achieve transparency. Figures 22 and 23 compare the performance of Nd³⁺ and Yb³⁺ under several pump conditions.

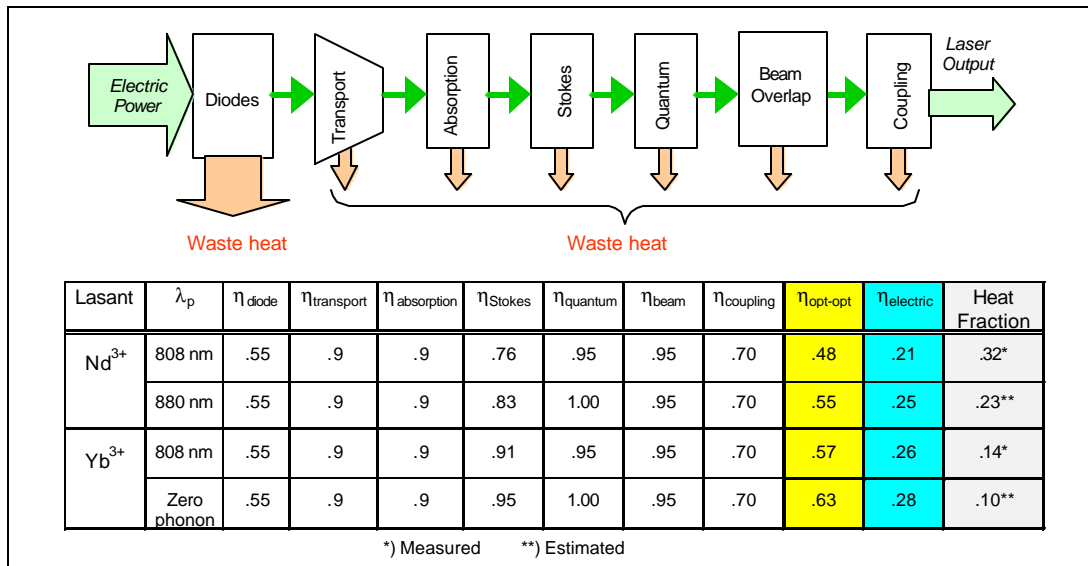


Figure 20: Typical efficiencies in a disk laser for Nd and Yb

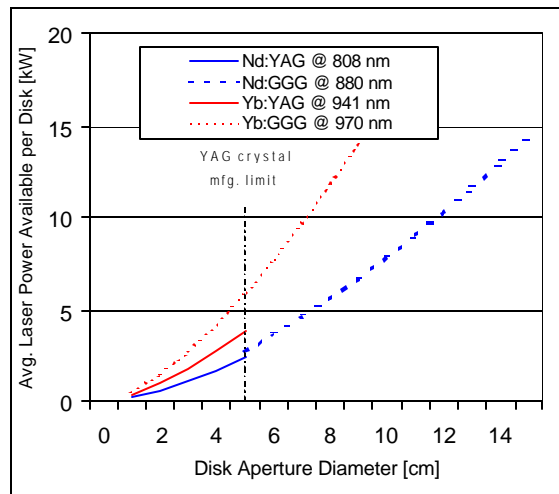


Figure 21: Power scaling of CAMIL disk using Nd and Yb lasers doped into YAG and GGG and operated under several pump conditions

Composite Disk

In side-pumping architecture, perimeter edge of the disk receiving pump radiation is susceptible to overheating and, as a result, to excessive thermal stresses. Drawing on our previous experience in designing end-pumped rod lasers [2] we designed a composite disk with a central doped section and undoped flared peripheral sections attached by diffusion bonding. Such a composite disk has several advantages. First, it facilitates improved coupling between the pump diodes and the doped portion of the disk. Second, its tapered profile and curved input surfaces additionally concentrate incident pump radiation. Third, the undoped edge draws heat away from the peripheral edge of the doped disk and conducts it to the substrate. This avoids excessive thermal stresses and perturbation of the optical phase front near the edge of the disk, Figure 22. Finally, the undoped optical medium is shaped to trap ASE rays and/or channel them outside the disk, which greatly reduces feedback to parasitic oscillations.

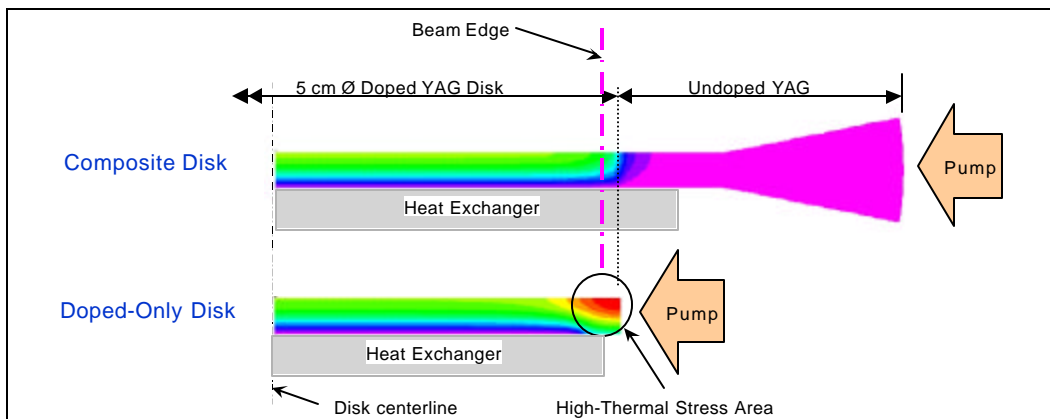


Figure 22: Comparison of composite and doped disk-only temperature distributions showing that the undoped edge draws heat away from disk edge and avoids excessive temperature and stresses

Pump and Gain Uniformity

Portions of the gain medium disk closest to the pump source are susceptible to being pumped more intensely than portions further away. Non-uniform deposition of pump energy can result in non-uniform gain and loss of beam quality. Achieving high uniformity of gain becomes even more challenging in view of ground state depletion by pump radiation and gain saturation by incident laser.

Happily, the architecture of side-pumped CAMIL can effectively compensate for such effects and produce a uniform gain profile over a large portion of the disk area. Side-pumping exploits the natural divergence of pump diodes to achieve spatially uniform pumping. Beamlets produced by individual laser diode elements in the circular array overlap inside the gain medium disk and their intensities are summed, Figure 23. Volumetric density of absorbed pump power produced by superposition of multiple beamlets depends on the power output and beamlet divergencies of individual diode elements, distance of the diode elements from the disk center, and density of ground-state ions in the gain medium.

Figure 23 shows examples of how the radial variation of small-signal gain is affected by choices of diode divergence (in the plane parallel to disk face) and diode distance from the disk center for exponentially absorbing laser medium. Trend seen in these graphs can be explained as follows. Low-divergence diode beamlets overlap mainly in the central portion of the disk, which leads to an intensity maximum there. High-divergence diode beamlets overlap in much of the disk volume, but their intensities decrease rapidly both due to spreading and absorption. This causes the maximum pump intensity near the perimeter of the disk that is closer to the diodes.

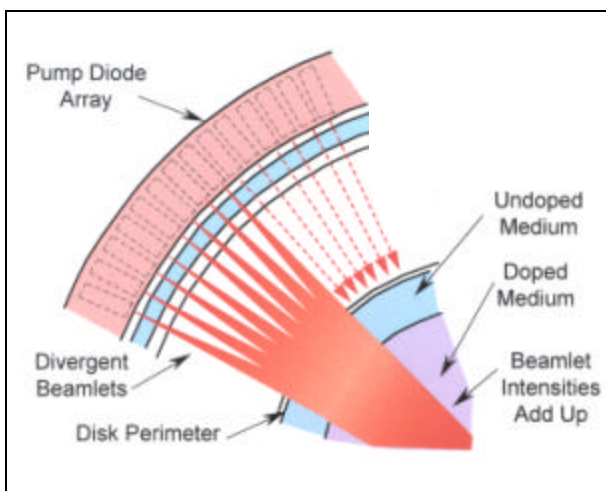


Figure 23: Superposition of beamlet intensities

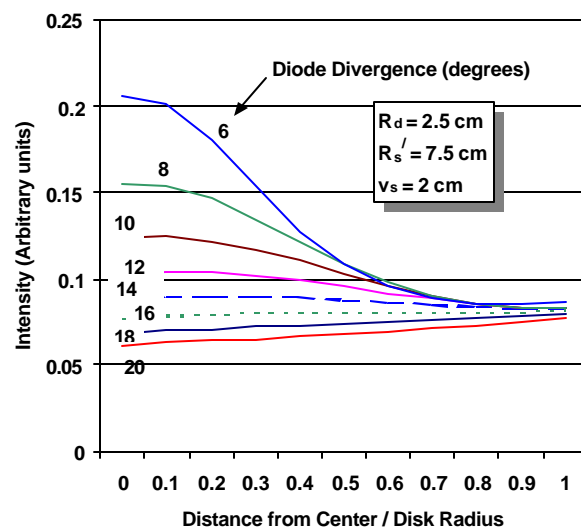
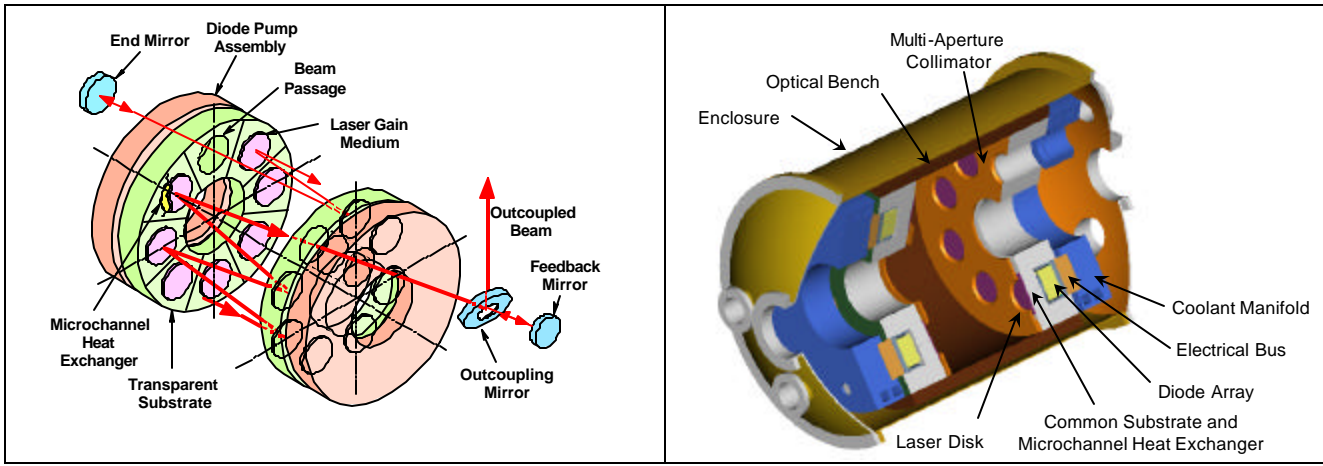


Figure 24: Pump power density profiles calculated for certain choice of disk and diode parameters [24]

8. ENGINEERING CONCEPT

We already noted that a laser oscillator can be constructed by placing multiple disk modules inside an unstable resonator. Figure 25 shows our approach to engineering a laser oscillator based on the face-pumped CAMIL concept. To achieve a high-degree of compactness we developed a resonator with axisymmetric layout shown in Figure 25a. The number of components is reduced and assembly is simplified by mounting several disks onto a common substrate containing internal coolant manifolds. Two such substrates can be positioned face-to-face on an optical bench and equipped with resonator mirrors. Figure 25b shows a laser device assembly with a cylindrical optical bench that provides sufficient stiffness to maintain optical alignment under operational dynamic loads. The assembly is further provided with power buses, and electric and fluid connections. The resonator assembly is placed inside an enclosure protecting the components and maintaining the pressure required for disk attachment. A 40-kW average power laser operating in a quasi-cw mode may use fourteen 7-cm Nd:GGG disks diode-pumped with 808 nm light in 200 μ s at 500-Hz pulse repetition rate (i.e., duty factor $\psi = 10\%$). Note that if the Nd:GGG disks were replaced by Yb:GGG disks side-pumped at 970 nm, the average power output of this device could increase by as much as 3-fold.



a) Axisymmetric resonator concepts showing multiple disks mounted on a common substrate

b) Engineering concept

Figure 25: Engineering concept for a face-pumped CAMIL for 5 to 50 kW average laser power

9. APPLICATIONS

High and ultrahigh-average power SSL with good beam quality enhance many existing industrial processes and enable some new applications. SSLs are replacing CO₂ lasers in critical manufacturing processes such as cutting and welding. Despite their higher capital cost, SSL offer operational flexibility with multi-kilowatt beams delivered by optical fibers. SSLs will soon match industrial CO₂ lasers in power and beam quality, and their shorter wavelength already permits an order of magnitude tighter beam focus. Resulting increase in incident beam intensities enables new processing regimes. Laboratory experiments [37] show that such high-brightness SSLs are instrumental for production of clean cuts and deep penetration welds in thick plates that are encountered in production of heavy equipment, shipbuilding, and construction. As seen in Figure 26, deep penetration welds produced by high-brightness SSLs have a very small heat affected zone and generally, resemble the more expensive electron beam welds. Furthermore, 20- to 60-kW beams delivered through optical fibers are also required for thick section cutting in nuclear decontamination and decommissioning [38]. Other emerging applications for UHAP SSL include rock drilling for oil and gas exploration [39], laser power beaming, orbital debris removal [40], and laser propulsion.

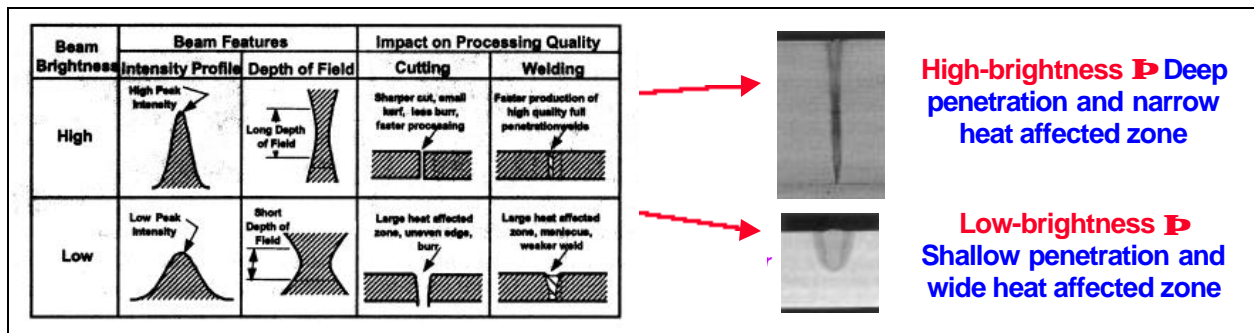


Figure 26: High-brightness SSL enable precision cutting and deep-penetration welding (photos courtesy of Caterpillar Corp.)

10. CONCLUSION

We presented a concept and scaling considerations for CAMIL, a large aperture disk laser in active mirror configuration. CAMIL uses a laser disk attached to a rigid cooled substrate that maintains it in an optically flat condition. This novel approach permits operation at HAP while delivering good BQ. CAMIL laser disk can be

used as a gain element in a wide variety of laser oscillator and power amplifier configurations. Applications enabled by HAP high-brightness SSL such as CAMIL includes thick section cutting, deep-penetration welding, cutting and welding of aluminum in the manufacture of aircraft, and drilling of cooling holes in manufacture of jet engines.

ACKNOWLEDGEMENTS

Author is indebted to Charlie Turner Jr., Robert Rice, and Petras Avizonis of The Boeing Company and Georg Albrecht of the Lawrence Livermore National Laboratory for many useful discussions. He also thanks Rashmi Shah and Tom Endo of The Boeing Company for performing finite element thermal analyses results of which are shown in Figures 16, 17, and 22.

ACRONYMS

1-D	- One dimensional	HAP	- High-average power
$\nabla_{\perp}T$	- Transverse temperature gradient	LLNL	- Lawrence Livermore National Laboratory
AMA	- Active mirror amplifier	MOPA	- Master oscillator - power amplifier
ASE	- Amplified spontaneous emission	SP	- Side pumping
BQ	- Beam quality	SSL	- Solid-state laser
CAMIL	- Compact active mirror laser	UHAP	- Ultrahigh-average power
FP	- Face pumping		

REFERENCES

1. W. Kerchner, "Solid-state laser engineering," chapter 7: "Thermo-optic effects and heat removal," 5th edition, Springer-Verlag, New York, NY, 1999
2. R. Beach et al., "High-average power diode-pumped Yb:YAG lasers," UCRL-JC-133848, September 1999
3. W.S. Martin and J.P. Chernoch, US Patent 3,633,126 (1972)
4. R.J. St. Pierre et al., "Active tracker laser (ATLAS)," *IEEE J. of Selected Topics in Quant. Electr.*, vol. 3, no. 1, February 1997
5. J. Machan et al., "High-brightness, 3 kW diode-pumped, industrial laser," in *Proc. from ICALEO'1999*, San Diego, CA, November 15-18, 1999, 143-148
6. H. Ineyan and C.S. Hofer, "End-pumped zigzag slab laser gain medium," US Patent 6,094,297
7. R. Beach et al., "Delivering pump light into a laser gain medium while maintaining access to the laser beam," US Patent 6,222,872
8. T.S. Rutherford, "Edge-pumped quasi-three-level slab lasers: design and power scaling," *IEEE J. of Quantum Electron.*, vol. 36, no. 2, 205-219, 2000
9. G. F. Albrecht, B. Comaskey, and L. Fury, "A 1.4 kJ Solid-state power oscillator with good beam quality," UCRL-JC-115127, August 1993
10. L. Hackel, "The Mercury laser, a diode-pumped solid-state laser driver for inertial fusion, is activated," UCRL-TB-136126-01-02, February 2001
11. B. Dane, L. Flath, M. Rotter, S. Fochs, J. Brase, and K. Bretney, "Army solid-state laser program: Design, operation, and mission analysis for heat capacity laser," in *Technical digest from the 14th Annual Solid-State and Diode Laser Technology Review*, held in Albuquerque, NM, May 20-25, 2001
12. G. Albrecht, S. Sutton, H. Robey, and B. Freitas, "Flow, heat transfer, and wavefront distortion in a fas-cooled disk amplifier," UCRL-100420, January 1989
13. J. L. Emmett, W. F. Krupke, and J. B. Trenholme, "The future development of high-power solid-state laser systems," UCRL-53344, November 1982

14. J. A. Abate, L. Lund, D. Brown, S. Jacobs, S. Reformat, J. Kelly, M. Gavin, J. Waldbillig, and O. Lewis, "Active mirror: a large-aperture medium-repetition rate Nd:Glass amplifier," *Appl. Opt.* Vol. 20, no. 2, 351, 1981
15. D. C. Brown, J. H. Kelly, and J. A. Abate, "Active-mirror amplifiers: Progress and prospects," *IEEE J. of Quantum Electron.*, vol. 17, no. 9, 1755, 1981
16. D. C. Brown, R. Bowman, J. Kuper, K. K. Lee, and J. Menders, "High-average power active-mirror amplifier," *Applied Optics*, vol. 25, no. 5, pp. 612-618, March 1, 1986
17. J. H. Kelly, D. L. Smith, J. C. Lee, S. D. Jacobs, D. J. Smith, J. C. Lambropoulos, and M. J. Shoup III, "High-repetition rate Cr:Nd:GSGG active mirror amplifier," *Opt. Letters*, vol. 12, no. 12, pp. 996-998, 1987
18. Giesen, H. Hugel, A. Voss, K. Wittig, U. Brauch, and H. Opower, "Scalable concept for diode-pumped high-power lasers," *Appl. Phys. B* 58, 365-372, 1994
19. Stewen, K. Contag, M. Larionov, A. Giesen, and H. Hugel, "1-kW CW thin disk laser," *IEEE J. Selected Topics in Quantum Electr.*, vol. 6, no. 4, pp. 650-657, July/August 2000
20. L. Zapata, R. Beach and S. Payne, "Composite thin-disk laser scalable to 100 kW average power output and beyond", in the Technical Digest from the Solid State and Diode Laser Technology Review, held in Albuquerque, NM., June 5-8, 2000
21. M. M. Tedrow et al., "Characterization of a diode-pumped, 3.8-cm clear aperture, high-gain, active mirror amplifier using Cr:Nd:GSGG and Nd:GGG," in *Proc. Adv. Solid-State Laser Conf.*, Santa Fe, NM, 1992
22. "Laser modeling, design, fabrication, and testing," University of Rochester report to McDonnell Douglas Corporation, Contact No. Y1W202, August 1992
23. J. Vetrovec, "Active mirror amplifier for high-average power," SPIE vol. 4270 (2001)
24. J. Vetrovec, "Compact active mirror laser-CAMIL," SPIE vol. 4630 (2002)
25. J.L. Stapp and J. W. Bender, "Cooled transmissive optics technology," AFRL-DE-TR-2000-1004
26. M.A. Culpeper, J.P. Metz and J.L. Stapp, "Liquid-cooled transmissive optical component," in *Proc. from Solid-State and Diode Laser Technol. Rev.* held in Albuquerque, NM, June, 2000
27. J. Vetrovec, "Solid-state high-energy laser (SSHEL)," SPIE vol. 4632 (2002)
28. R. Lavi, S. Jackel, A. Tal, E. Lebiush, Y. Tzuk, and S. Goldring, "885 nm high-power diode end-pumped Nd:YAG laser," *Optics Comm.*, 195, pp. 427-430, August 2001
29. S. Chenais et al., "Diode-pumped operation of Yb:GGG laser," *proc. CLEO 2001*
30. J. Vetrovec, "Active mirror amplifier system and method for high-average power laser system," US patent no. 6,339,605 (2002)
31. Oliver Meissner, Onyx Optics Inc., Dublin, CA, communications
32. W. Kerchner, "Solid-state laser engineering," chapter 2: "Properties of solid-state materials," 5th edition, Springer-Verlag, New York, NY, 1999
33. G.T. Liu et al., "Reliable 20 W cw operation of 880 nm laser arrays with aluminum-free active regions," *proc. CLEO 2001*
34. G.T. Liu et al., "Performance and reliability of 20W diode laser bars at 880 nm," *proc. Solid-State and Diode Laser Technology Review*, Albuquerque, NM, May 21-24, 2001
35. W. F. Krupke, "Ytterbium solid-state lasers- the first decade," *IEEE J. on Selected Topics in Quantum Electron.*, vol. 6, no. 6, 1287-96, November/December 2000
36. H. Qui et al., "The influence of Yb concentration on laser crystal Yb:YAG," *Materials Letters* 3439 (2001)
37. J. Machan et al., "High-brightness, 3 kW diode-pumped, industrial laser," in *Proc. from ICALEO'1999*, San Diego, CA, November 15-18, 1999, 143-148
38. J. Vetrovec, M. Hallada, S. Seifert, and R. Walter, "Chemical oxygen-iodine laser for dismantlement of nuclear facilities," in *Proc. from ICALEO 1999*, November 15-18, 1999
39. D.G. O'Brien, R.M. Graves and E.A. O'Brien, "Star wars laser technology - the future for petroleum well drilling and completions," in *Proc. from ICALEO 1998*, November 16-19, 1998
40. C.R. Phipps, "Orion physics overview," in *Proc. from Lasers'96*, Portland, OR, Dec. 2-6, 1996